Solid State X-Ray Detectors for Digital Mammography

Justin M. Henry, Martin J. Yaffe, Bo Pi[1], John Venzon[2], Frank Augustine[3], and Tumay O. Tumer[1]

Department of Medical Biophysics, University of Toronto,
Imaging Research, Sunnybrook Health Science Centre,
2075 Bayview Avenue, Toronto, Ontario, M4N 3M5

[1] NOVA R&D, Inc., Riverside, CA
[2] Santa Barbara Research Center, Goleta, CA
[3] Augustine Engineering, Encinitas, CA

ABSTRACT

In conventional mammography, x-rays transmitted through the breast are converted to light in a phosphor screen, and the light exposes a film emulsion. The information in the image is degraded in this detector due to limitations in the screen and film. Photodiode arrays can convert the x rays directly into charge and overcome these problems.

A preliminary investigation of a thick crystalline silicon photodiode array as a solid state digital detector was performed. The prototype device consisted of a 300 μm thick, 256 x 256 photodiode array of 30 x 30 μm^2 pixels. The array was hybridized to two different readout structures for evaluation purposes, one structure being used for imaging and the other for single pixel experiments. Imaging performance, such as linearity, resolution and noise were measured and used to predict the performance of a proposed clinical version of the prototype.

Results show the detector response to be linear over the range of exposures required for mammography, the modulation transfer function (MTF) to be superior to that of screen-film detectors, and the noise to be dominated by x-ray quantum fluctuation. Based on results from the prototype devices, we predict that the detective quantum efficiency (DQE) of the clinical design will be significantly higher than that of a screen-film detector for all spatial frequencies of interest.

1. INTRODUCTION

Our hypothesis is that by providing a more sensitive means of detecting disease, digital mammography will facilitate the reduction of mortality from breast cancer. Image acquisition and image display are the two main areas where digital mammography can improve sensitivity and specificity. In screen-film detectors, the film performs both functions, resulting in inevitable tradeoffs in design. Each can be optimised independently by separating the two functions in digital mammography. In addition, image processing and computer aided diagnosis may also prove advantageous[1]. We are investigating a solid state digital detector that will not only overcome the limitations of a screen-film detector, but will also overcome some of the limitations many proposed digital detectors have.

The current mammographic technique uses an x-ray spectrum with energies in the range of 15 keV to 35 keV to irradiate the compressed breast. The detector has a field of view (FOV) of 24 cm by 30 cm and is placed behind the breast at 60 cm from the x-ray source (focal spot). The screen-film detector structure is shown in Figure 1. It consists of a settled phosphor screen in contact with a film emulsion layer. The screen absorbs the x rays transmitted through the breast and converts them into light, which exposes the film. It is a very simple and compact way to capture and store the image. There are, however, limitations in the film and screen. The inherent sigmoidal response curve of film to light limits displayed contrast in both the thin and dense portions of the breast[2], and the film emulsion grain size is the dominant source of noise at higher spatial frequencies[3]. The screen degrades resolution due to the spread of light before it escapes, and has a limited quantum efficiency, η, since its thickness is limited to minimize this blur. The screen also adds noise to the system due to variations in the amount of light emitted and escaping per interacting x-ray[4]. An anti-scatter grid is used to prevent degradation in contrast and signal-to-noise

0-8194-1780-7/95/$6.00

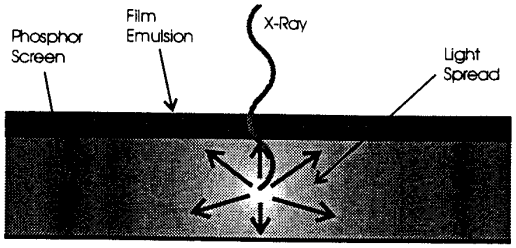

Figure 1. Screen-film detector.

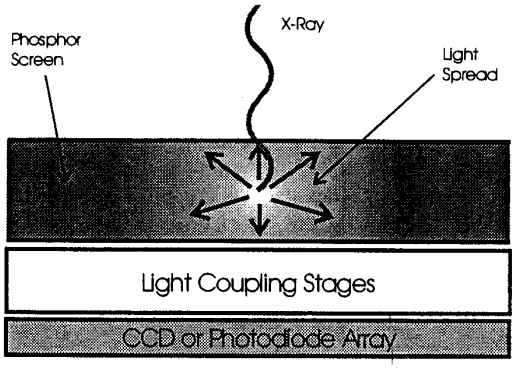

Figure 2. Generic "light conversion" digital detector.

ratio (SNR) due to x rays scattered in the breast. This, however, necessitates an increase in dose to the breast of 2.5 to 3 times. This is because the inefficient grid removes both scattered and primary x rays, and the film requires a sufficient amount of light to obtain proper optical density.

Figure 2 shows a generic "light conversion" digital detector. It is shown for comparison since several digital detectors use this approach. A phosphor screen is still used to absorb incident x rays and create an optical image. This is recorded using a photoelectronic detector such as a CCD or photodiode array. Although coupling can be by direct contact[5], it is more typical to use a lens or fibre optic taper[6] to reduce the image size to that of the photoelectronic detector. The main advantage of this type of system is its linear response to exposure. Recorded contrast is not limited in the thin and dense portions of the breast. Displayed contrast can be digitally manipulated while the image is viewed on a computer screen to reveal subtle density differences in all portions of the breast. In addition, film grain noise is eliminated.

This type of detector still suffers, however, from the limitations of the settled phosphor screen mentioned above. An additional problem is that due to losses in light in the coupling stages, a secondary quantum sink can exist at higher spatial frequencies. This means that the noise in the image is not dominated by the inherent quantum noise in the x rays incident on the detector at all spatial frequencies of interest[7]. Some work, however, has been done with CsI(Tl) screens in an attempt to overcome these problems[8].

Figure 3 shows the solid state detector concept under investigation. This detector is composed of a thick depletion photodiode array layer electrically coupled to a readout layer. The x rays are absorbed in the photodiodes and their energy is converted directly into electron-hole (e-h) pairs. The photodiodes are reverse-biased by applying a positive voltage to the n electrode with respect to the p+ electrodes. This creates an electric field in the vertical direction. The e-h pairs are swept apart to the surfaces by the electric field, electrons to the top and holes to the bottom surface.

Many of the film and screen limitations can be overcome with the solid state detector. As with the "light conversion" digital detector, the solid state detector's response is linear with exposure, so contrast is independent of breast thickness. Film grain noise is also removed. The replacement of the screen, however, has additional advantages.

The influence of the electric field has two effects.

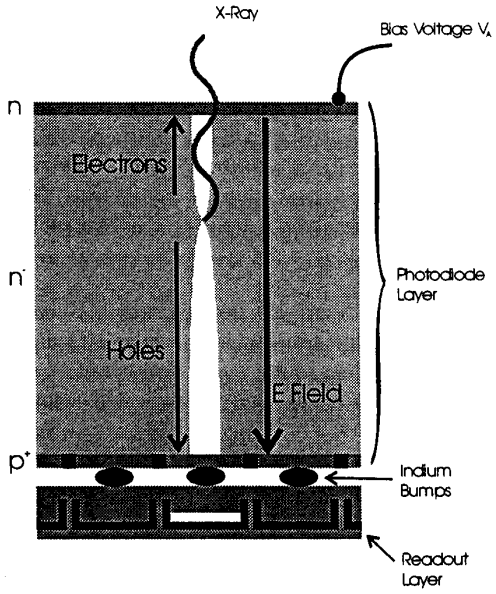

Figure 3. Solid state digital detector.

First, unlike the light in the phosphor screen which diffused in all directions before exiting, the charge is swept to the surface before undergoing significant lateral diffusion. This means that the resolution does not depend strongly on the thickness of the photodiode layer so it can be made thick to improve quantum efficiency. In addition, since the MTF is not a strong function of the depth of x-ray interaction, signal and quantum noise are transferred in a similar manner, and the DQE is not severely degraded. Secondly, the electrons and holes are separated by the electric field and so the chance of recombination is small. This minimizes fluctuations in the amount of charge collected per x-ray, thereby reducing noise.

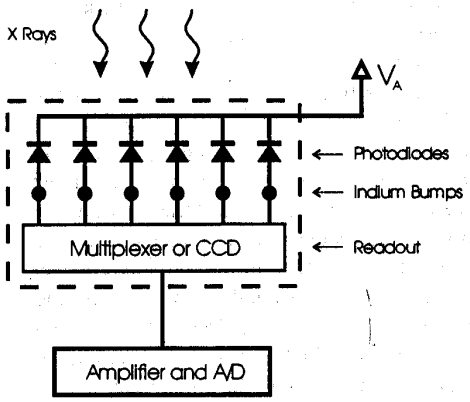

Figure 4. Electrical equivalent of the photodiode-readout hybrid.

The amount of energy required to create one e-h pair in semiconductors (W_{ehp}) is very low. This is advantageous since a large number of e-h pairs are created per interacting x-ray. For crystalline silicon, for example, W_{ehp} is 3.6 eV. A 20 keV x-ray will produce over 5500 e-h pairs. This eliminates the secondary quantum sink that can exist in a "light conversion" digital detector when the coupling efficiency is poor and typically only about 10 electrons are produced in the detector per interacting x-ray[6].

The thick photodiodes can introduce electronic noise due to random fluctuations in the amount of thermally generated e-h pairs, but this can be reduced by cooling and obtaining extremely pure semiconductor materials. High purity wafers, however, are typically not available in diameters larger than 100 mm. In addition, it is difficult to fabricate large area, thick photodiode arrays. The detector must therefore be used in a scanned-slot configuration to cover the full FOV (see Section 3). This has the benefit of efficiently reducing scatter, allowing elimination of the grid[9] or use of higher efficiency antiscatter devices[10].

This paper contains preliminary results of investigations performed with small area detectors. Once the important design and operation parameters have been determined from our results, larger area and thicker detectors will be fabricated and tested.

2. PHOTODIODE - READOUT ARRAY HYBRID

The solid state detector is composed of two layers, the thick photodiode array layer, and the readout layer. Figure 3 shows the physical construction, while Figure 4 shows the equivalent electrical circuit. The two layers are joined into one hybrid detector using indium bump bonds. The indium simply serves as an electrical connection between the two layers. The detector is built as a hybrid so that each layer can be designed, optimised and constructed separately.

The photodiode layer that was investigated is composed of crystalline silicon. Silicon was chosen for this preliminary investigation because it is available at high purity, and its fabrication technology is very advanced. Silicon, unfortunately, has a low atomic number of 14 so its linear attenuation coefficient is poor. It must be made very thick to achieve acceptable quantum efficiency. Figure 5 shows the quantum efficiency of a typical mammographic phosphor screen (31.7 mg/cm^2 Gd_2O_2S), a 300 μm and 1.5 mm thick silicon photodiode. The 300 μm thick photodiode has quite low quantum efficiency while that of the 1.5 mm photodiode is comparable to the phosphor screen in the mammographic energy range

The silicon is lightly n doped (n^-). Due to its low level of doping, it is often referred to as the "intrinsic region". The top surface is n-type while the bottom surface is p-type. This forms a positive - intrinsic - negative (PIN) photodiode. The lower surface is pixellated using a SiO_2 mask while the top surface acts as a common electrode.

Two prototypes supplied by Santa Barbara Research Center (a subsidiary of Hughes Aircraft) were used for evaluation purposes. Both had a 300 μm thick, 256 x 256 photodiode array layer with 30 x 30 μm^2 pixels. One detector had a direct readout layer while the other had an imaging readout layer. The purpose of the readout layer is to collect the charge created in the photodiodes. An equally important task that it must perform is the efficient organization of the information. For a mammographic detector of any reasonable area and pixel size, it is impractical to individually connect each photodiode to the external amplification and digitizing circuitry. The direct readout detector had a simple "fanout" layer in which a sampling of individual pixels were directly connected to the chip holder's pins, while the rest were connected to a common ground. This detector was used to investigate the operation of individual photodiodes and eliminated effects due to the readout scheme. The imaging detector had a more sophisticated readout layer. Each pixel had a charge storage element and was addressable using a multiplexing scheme. This detector was used to measure resolution and uniformity.

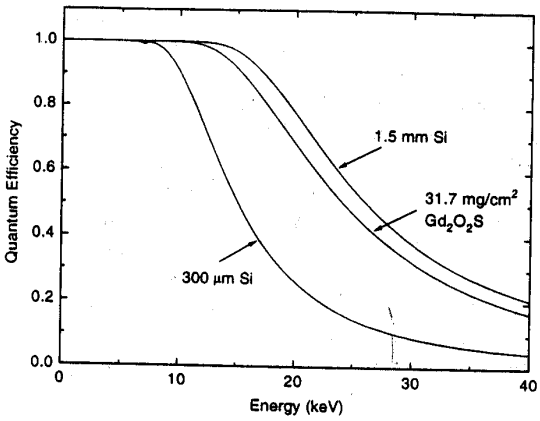

Figure 5. Quantum efficiency of a typical mammographic phosphor screen, a 300 μm and 1.5 mm crystalline silicon photodiode.

3. SCANNED SLOT CONCEPT

One limitation of using crystalline semiconductors for the photodiode layer is the difficulty in manufacturing them in large areas. To overcome this problem, we propose to use the detector in a scanned-slot configuration. Figure 6 shows the mechanical construction. A fanned x-ray beam scans the breast and is tracked by a long, thin hybrid detector. The readout layer operates in time delay integration (TDI) mode[11]. The scanned-slot configuration has excellent scatter reduction, thereby increasing contrast in the image without the need for an anti-scatter grid. This is because only a thin slot is irradiated at one time. The elimination of the grid could allow for a reduced dose to the breast.

One advantage of operating in TDI mode is the simplicity of the mechanical scanning system. Another advantage is that not every pixel need be functional. Each pixel in the image results from the integration of signal from many detector pixels. This significantly increases detector yield and reduces the cost.

As a starting point, we have estimated desirable performance specifications for a scanned-slot, digital mammography system. A scan over a 30 cm field will be performed in 6 seconds. The detector, with a 1.5 mm thick crystalline silicon photodiode layer, will be hybridized to a CCD layer, specially fabricated to have a large well capacity of 15 x 10^6 electrons. The charge generated in the photodiode will be split before entering the CCD so that the maximum x-ray signal can be accommodated without saturating the readout capacity. The hybrid will have 200 TDI stages (rows) with 50 x 50 μm^2 pixels. This results in an integration time of 0.2 s per pixel. For initial work the detector will be cooled to -10°C.

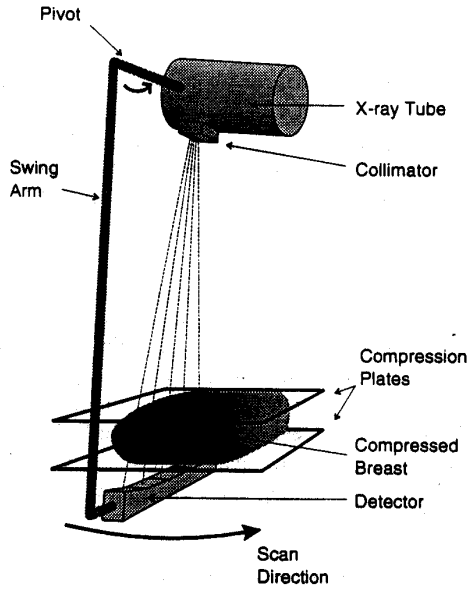

Figure 6. Scanned-slot configuration.

The thickness of the photodiode layer needs to be taken into account when constructing a long detector. As the thickness increases, x rays not normal to the surface may pass into adjacent pixels before being absorbed, resulting in reduced resolution. For a 1.5 mm thick detector 60 cm from the x-ray source, the lateral spread due to angular incidence can be as much as 600 μm at the edge of the 24 cm field of view. To overcome this problem, the detector assembly will be curved with a radius equal to the x-ray source-detector distance. This can be achieved by constructing the detector from many individual hybrid chips to approximate the curvature. It is difficult to place multiple chips end to end without any dead space, so a staggered approach will be taken as shown in Figure 7. The detector will scan side to side to prevent dead space along the chest wall. The length and width of each chip will be optimized by taking into account the geometric blur, scatter to slot-width ratio, tube heat loading, etc.

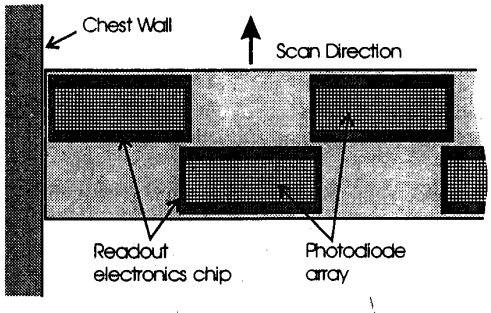

Figure 7. Staggered slot array for gapless imaging.

4. PROTOTYPE EVALUATION

Experiments were performed to determine the feasibility of a solid state hybrid detector. Since the evaluation devices were small and thin, the results were extrapolated to predict the performance of the proposed clinical detector described in Section 3.

4.1 Depletion width

When the photodiode array is reverse-biased, a "depletion" region forms at the p^+ - n^- boundary. This region is depleted of carriers (electrons or holes generated by thermal excitation) and has an electric field across it. As the reverse-bias voltage is increased, the depletion region grows into the n^- region until it reaches the n region[12]. At this point the photodiode is said to be fully depleted. If the reverse-bias voltage exceeds the depletion voltage, the depletion thickness does not grow significantly, but the electric field is increased thereby increasing charge collection efficiency.

It is important to ensure that the photodiode is fully depleted. Only e-h pairs generated within the depletion region have a high probability of being collected and so the effective thickness of the photodiode is determined by the depletion thickness. To measure the depletion region thickness, the capacitance of the photodiode can be monitored as the reverse-bias voltage is increased (C-V technique). The depletion width W is related to the capacitance C by

$$W = \frac{\epsilon_S A}{C} \qquad (1)$$

where ϵ_S is the semiconductor permittivity and A is the area of the photodiode. When the photodiode is fully depleted, the capacitance will not decrease with additional applied voltage. C-V measurements performed at Santa Barbara Research Center indicate that the prototype photodiode layer is fully depleted above 30 V reverse-bias.

4.2 Dark current

Thermal generation of e-h pairs in the depletion region causes a current to flow through the photodiodes in the absence of x rays. Two problems arise from this dark current: the filling of the readout storage elements and shot noise. Both effects can be minimized by reducing the dark current which can be done by reducing the operating temperature and increasing the purity of the photodiode. The choice of material will also effect the dark current. Silicon has a relatively large dark current at room temperature[13] due to its low band gap energy of 1.12 eV. It can, however, be processed to extremely high purities which tends to compensate for this disadvantage.

The dark current of the direct readout detector was measured as a function of reverse-bias voltage. Figure 8 shows the dark current per pixel. The increase in dark current as the bias voltage is increased is related to the increase in depletion thickness and increased charge collection efficiency.

Using these results, and taking into account the increased thickness and decreased temperature of the proposed detector, we expect 1 x 10^5 electrons will be collected in the CCD wells during the scan. This is less than 1% of the full well capacity.

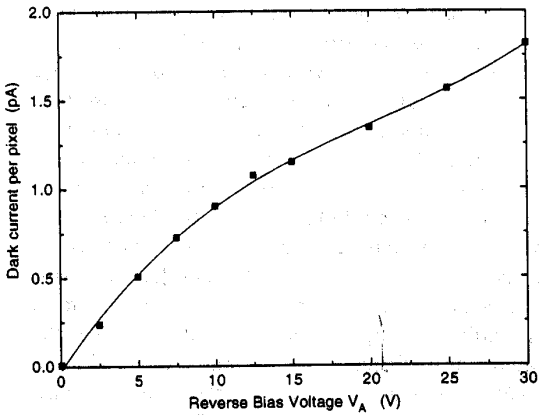

Figure 8. Dark current versus applied reverse-bias voltage.

4.3 Linearity

One of the main advantages of a solid state detector over the screen-film combination is that its response to exposure is linear. To investigate the response of the photodiodes, the direct readout detector was subjected to the range of expected exposure rates while the current generated in one pixel was measured. The detector was reverse-biased at 30 V and placed 30 cm from a tungsten target x-ray tube, operating at 27 kVp, with 0.13 cm Al total filtration. The tube current was used to vary the exposure rate.

The x-ray generated current is plotted versus exposure rate in Figure 9 with a straight line fit to the data. The response of the detector is linear, with a maximum deviation of 5% at high exposure rates. This could be due to recombination of e-h pairs at high charge density. Increasing the reverse-bias voltage should increase the charge collection efficiency and minimize this effect.

4.4 Resolution

The imaging detector was used to make resolution measurements. It was cooled to -10°C using a Peltier device and was maintained in a nitrogen environment to prevent ice forming. Images of lead test patterns, placed 1.5 cm from the detector, were made using a tungsten x-ray source operating at 35 kVp. To minimize focal spot blur due to the 1 mm focal spot size, and magnification due to the 1.5 cm object-to-image distance (limited by the detector housing), the detector was placed 107 cm from the x-ray focal spot. On this detector the storage element associated with each pixel on the readout layer had a low capacity. Few x-rays were required to reach saturation and this resulted in very noisy images due to x-ray quantum statistics. To overcome this limitation in the prototype device, ten images were acquired and added together. Images were also made in the dark and with uniform x-ray illumination. This allowed for the characterization of pixel to pixel variations. These data were used to correct the test pattern images.

Figure 10 is an image of a 2° star pattern. The lines at the centre, which correspond to approximately 13 lp/mm, are clearly visible. This image also shows that after corrections, an artifact free image can be obtained. An image of a bar pattern is shown in Figure 11. Here 16 lp/mm are visible. Some artifacts remain in this image due to saturation of the prototype detector in some areas.

The MTF(f) was also measured by imaging a high contrast edge (a polished tantalum plate). To minimize the effects of aliasing in the measurement, the edge was slanted slightly with respect to the detector's columns, and the image was processed to obtain an

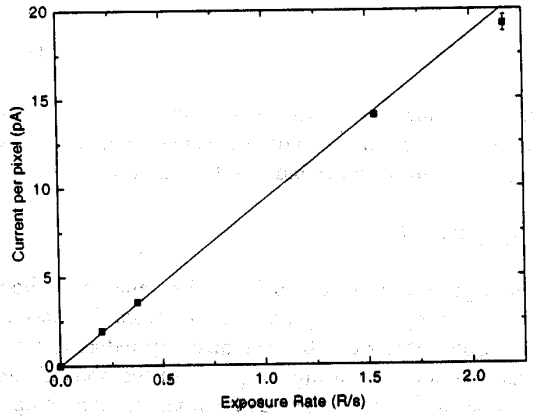

Figure 9. Generated current versus exposure rate.

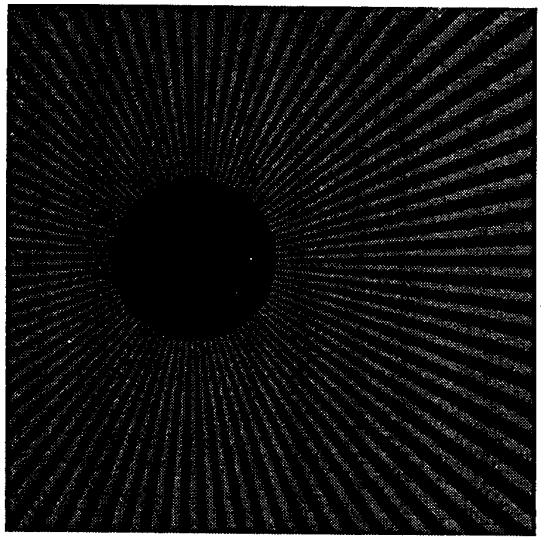

Figure 10. Image of lead star pattern.

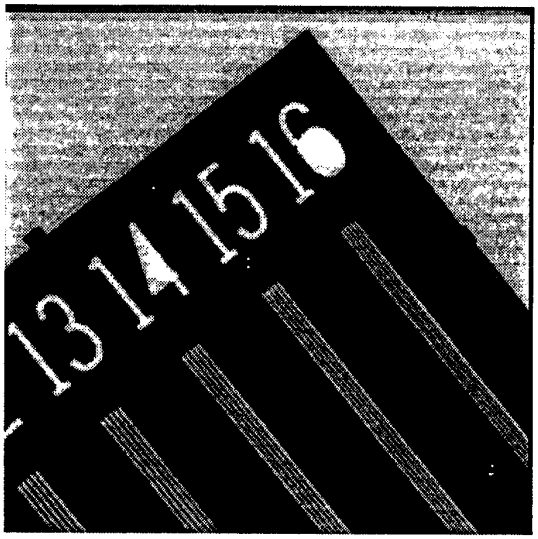

Figure 11. Image of lead bar pattern.

over-sampled edge spread function (ESF) which was used to calculate the pre-sampled MTF(f)[14]. The MTF(f) of the photodiode array is compared to the MTF(f) of a state of the art screen-film detector in Figure 12. The photodiode array has a significantly higher MTF(f). It is, however, lower than the maximum achievable with a 30 μm pixel width, namely the aperture response. This decrease can be partially accounted for by focal spot blur[15], and by lateral charge spread in the depletion region[16]. To overcome these effects, subsequent measurements will be made with a small focal spot, low magnification, and increased reverse-bias voltage. Increasing the bias voltage will decrease the lateral charge spread by reducing the charge collection time. Radiation transport models developed in our laboratory[16] describe effects that degrade resolution, such as lateral charge diffusion within the photodiode layer. Using these models, we predict the MTF(f) of a 1.5 mm photodiode array will be significantly better than the screen-film MTF(f).

4.5 Noise

As with all imaging systems, noise introduced by the detector reduces the detectability of small, low contrast structures in the breast. Dark current noise measurements made with the prototype detector (adjusted to take into account the proposed detector's increased thickness, charge splitting approach and reduced temperature) were compared with estimates of the noise introduced by a CCD layer, amplifier stages and A/D.

Shot noise per pixel, σ_{dark}, is related to the dark current by

$$\sigma_{dark} = (q^{-1} J_{dark} A_{pixel} t_I)^{1/2} \qquad (2)$$

where q is the electron charge, J_{dark} is the dark current density, A_{pixel} is the pixel area and t_I is the integration time. Based on the dark current results in Section 4.2, the dark shot noise of the proposed detector should be $\sigma_{dark} \approx 316$ electrons. For this integration time and temperature, we estimate σ_{dark} will dominate over the other electronic noise sources[11]. This is primarily due to the large depletion volume of the photodiode from which thermally generated e-h pairs are collected.

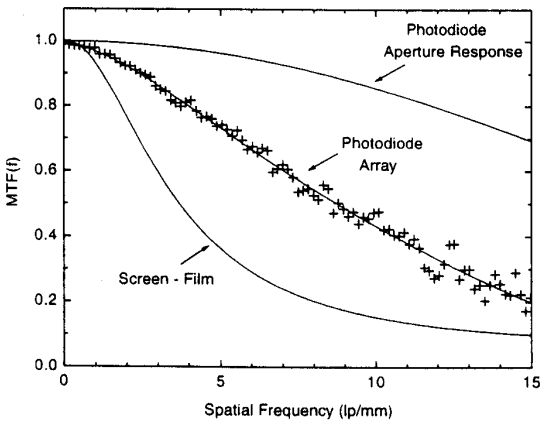

Figure 12. MTF of a screen-film system and the 300 μm thick prototype device.

The x-ray quantum noise can be converted to an equivalent noise in the generated charge for comparison with the dark shot noise. Assuming noiseless gain in the photodiode (a good assumption since the Fano factor is small[17]), the equivalent noise is

$$\sigma_{EQ} = G\sigma_Q = G\sqrt{\eta N_Q} \tag{3}$$

electrons, where σ_Q is the quantum noise, G is the gain of the photodiode (~5500 electrons per 20 keV x-ray) and N_Q is the number of x rays incident on the detector. Beneath a very thick, dense breast, an exposure of 1 mR can be expected. This corresponds to only 96 x-ray quanta detected per pixel, and σ_{EQ}≈5400 electrons after charge splitting. Therefore, even at these low exposure levels, quantum noise dominates.

4.6 Dynamic Range

With dominant shot noise of 316 electrons, dark charge of 1 x 10^5 and a full well capacity of 15 x 10^6 electrons, the dynamic range is estimated as ~ 47 x 10^3.

4.7 DQE

The DQE(f) measures how well the signal to noise ratio (SNR) propagates through a system and is defined as

$$DQE(f) = \frac{SNR_{out}(f)^2}{SNR_{in}(f)^2} \tag{4}$$

The $SNR_{in}(f)$ is dictated by the exposure used to make the image. The $SNR_{out}(f)$ is reduced by the quantum efficiency, the difference in the way the signal and noise pass through the system, and by added noise. At best DQE(f) = η.

The method of Nishikawa and Yaffe[18] was used to estimate the DQE(f) of the proposed solid state detector. DQE(f) can be factored into four components,

$$DQE(f) = \eta\ A_S\ R_N(f)R_C(f) \tag{5}$$

where A_S is the scintillation efficiency (Swank factor)[4]. $R_N(f)=W_Q(f)/W_T(f)$, the ratio of the x-ray quantum noise power to the total noise power. $R_C(f)=[MTF(f)/NTF_Q(f)]^2$ and describes the difference in the transfer efficiency of signal [MTF(f)] and quantum noise $[NTF^2_Q(f)=W_Q(f)/W_Q(0)]$.

For the proposed detector with a 1.5 mm thick photodiode layer, η≈0.7. Because of its narrow pulse height distribution, A_S≈1. $R_N(f)$ is also expected to be close to one, even at high spatial frequencies since $W_T(f)≈W_Q(f)$ due to the large gain and low levels of added noise. $R_C(f)$ is reduced from one if the MTF(f) is a function of depth of x-ray interaction. Our models of energy transport in the photodiode layer predict this dependency to be small in the proposed detector resulting in a $R_C(f)$≈1. Combining these factors in Eq. (5), the DQE(f) is expected to be 70% at zero spatial frequency, and relatively flat to above 15 lp/mm. In current mammographic systems, DQE is typically 30% to 40% at zero spatial frequency and drops to less than 1% at 15 lp/mm [3]. This is primarily due to three factors: (1) fluctuations in the amount of light produced in the screen (A_S≈0.65)[3], (2) a strong dependence of MTF(f) on x-ray interaction depth in the screen ($R_C(f)$ drops rapidly with spatial frequency)[17], and (3) the dominance of film grain noise at higher spatial frequencies (ie. $R_N(f)$ decreases)[3].

4.8 Radiation damage

Both the photodiode layer and CCD readout layer can be optimized separately for radiation hardness due to the hybrid nature of the device. Silicon PIN diodes are naturally radiation hard[19]. CCDs are more susceptible to radiation damage. In the hybrid detector, however, the CCD is shielded by the photodiode layer and so receives a significantly lower dose. It will, however, be designed and fabricated using one of the radiation-hard manufacturing techniques. The effects of radiation damage during the lifetime of the device should therefore not be significant.

5. SUMMARY

Based on measurements made on prototype devices, the proposed clinical solid state digital detector will meet performance criteria of an improved mammographic detector. In order to have acceptable quantum efficiency, a silicon photodiode layer of thickness 1.5 mm is desirable. Increased electric field strengths compared to those used in the prototype detectors will yield increased resolution and charge collection efficiency. The detector will likely require cooling to prevent the dark current from filling the CCD wells. The charge from the photodiodes will also be reduced through splitting, so that only a fraction is collected, to prevent CCD well saturation at maximum exposures. The quantum noise will be the dominant source of noise, even at low exposure levels and high spatial frequencies.

The hybrid construction of the detector allows other photodiode materials to be used in place of crystalline silicon, for example, to provide lower dark current or greater x-ray attenuation for specific imaging tasks.

6. ACKNOWLEDGMENTS

This work was supported by National Institutes of Health Grant No. CA66015. We gratefully acknowledge Santa Barbara Research Center for supplying the evaluation devices, and Gordon Mawdsley for technical support. The first author is supported by a University of Toronto Open Scholarship.

7. REFERENCES

1. H.P. Chan, K. Doi, S. Galhotra, C.J. Vborny, H. MacMahon, and P.M. Jokich, "Image feature analysis and computer-aided diagnosis in digital radiography. 1. Automated detection of microcalcifications in mammography", Med. Phys., **14**, pp. 538-548, 1987.

2. D.B. Plewes, J.M. Sabol, I. Soutar, A. Chevrier, and R. Shumak, "Role of equalisation mammography of dense breasts", Med. Biol. Eng. & Comput. (in press).

3. R.M. Nishikawa, and M.J. Yaffe, "Signal-to-noise properties of mammography film screen systems", Med. Phys., 12(1), pp. 32-39, 1985.

4. R.K. Swank, "Absorption and noise in x-ray phosphors", J. Applied Physics, 44, pp. 4199-4203, 1973.

5. L.E. Antonuck, J. Yorkston, W. Huang, J. Boudry, and E.J. Morton, "Large area, flat-panel a-Si:H arrays for x-ray imaging", Proc. SPIE, **1896**, pp. 18-29, 1993.

6. A.D.A. Maidment, and M.J. Yaffe, "Analysis of the spatial-frequency-dependent DQE of optically coupled digital mammography detectors", Med. Phys. 21(6), pp. 721-729, 1994.

7. I.A. Cunningham, M.S. Westmore, and A. Fenster, "Visual impact of the non-zero spatial frequency quantum sink", Proc. SPIE, **2163**, pp. 274-283, 1994.

8. I. Jujieda, G. Cho, J. Drewery, T. Gee, T. Jing, S.N. Kaplan, V. Perez-Mendez, and D. Wildermuth, "X-ray and charged particle detection with CsI(Tl) layer coupled to a-Si:H photodiode layers", IEEE Trans. on Nucl. Sci., Vol. 38 (2), pp. 255-262, 1991.

9. M.J. Yaffe, R.M. Nishikawa, A.D.A. Maidment, and A. Fenster, "Development of a digital mammography system", Proc. SPIE, **914**, pp. 182-188, 1988.

10. R. Fahrig, J.G. Mainprize, and N. Robert, "Performance of glass fiber antiscatter devices at mammographic energies", Med. Phys., 21(8), pp. 1277-1282, 1994.

11. D.W. Holdsworth, R.K. Gerson, A. Fenster, "A time-delay integration charge-coupled device camera for slot-scanned digital radiography", Med. Phys., 17(5), pp. 876-886, 1990.

12. S.M. Sze, *Semiconductor Devices, Physics and Technology*, pp. 75-83, John Wiley & Sons, New York, 1985.

13. G.F. Knoll, *Radiation Detection and Measurement, 2nd ed*, pp. 465-468, John Wiley & Sons, New York, 1989.

14. P.F. Judy, "The line spread function and modulation transfer function of a computed tomographic scanner", Med. Phys., 3(4), pp. 233-236, 1976.

15. E.L. Nickoloff, E. Donnelly, L. Eve, J.V. Atherton, and T. Asch, "Mammographic resolution: Influence of focal spot intensity distribution and geometry", Med. Phys., 17(3), pp. 436-447, 1990.

16. W. Que and J.A. Rowlands, "X-ray imaging using amorphous selenium: Inherent spatial resolution", Med. Phys. (in press).

17. G.F. Knoll, *Radiation Detection and Measurement, 2nd ed*, 340, John Wiley & Sons, New York, 1989.

18. R.M. Nishikawa and M.J. Yaffe, "Model of the spatial-frequency-dependent detective quantum efficiency of phosphor screens", Med. Phys., 17(5), pp. 894-904, 1990.

19. S.L. Shapiro, W. Dunwoodie, J. Arens, J. Gernigan, and S. Gaalema, "Silicon PIN diode array hybrid for charged particle detection", Nucl. Instr. and Meth. A275, 580, 1989.